Non-Newtonian Flow in Polymer Systems with No Entanglement Coupling

Robert A. Stratton[1]

Mobil Chemical Company, Edison, New Jersey 08817.

Received February 7, 1972

ABSTRACT: The non-Newtonian viscosity of polymer melts and solutions under conditions of no entanglement coupling has been investigated. The characteristic shear rate for a given degree of viscosity loss has been found to be proportional to the first power of the concentration and the inverse first power of the molecular weight, in agreement with the Rouse terminal-relaxation time. It was shown that either the Takemura or Pao–Rouse theories can be used to predict the onset and course of non-Newtonian behavior of monodisperse polymers to within better than a factor of 2. Measurements made under high pressures have been successfully corrected to those obtaining under ambient pressure conditions. Anomalous die swells were shown to be the result of a small concentration of high molecular weight material in an otherwise monodisperse low molecular weight sample.

A number of theories have been proposed[2-5] to describe the flow of isolated polymer molecules in a continuous medium using the pearl-necklace model. Although several of these[2-4] predict non-Newtonian flow, Zimm[5] showed that a correct formulation of this model, with scalar preaveraged (or vanishing) hydrodynamic interactions, must give a gradient-independent viscosity. More recently, Fixman[6] showed that non-Newtonian viscosity is obtained if the hydrodynamic interactions are not prematurely averaged.

All of the theories mentioned[2-4] predict that the reduced viscosity $(\eta - \eta_s)/(\eta_0 - \eta_s)$ for different samples should be a universal function of the product of shear rate times a characteristic relaxation time[7] τ_R.

$$\tau_R = 6(\eta_0 - \eta_s)M/\pi^2 cRT \tag{1}$$

Still other theories[6,8-10] based on different models present $[\eta]/[\eta]_0$ as a function of a reduced shear rate β.

$$\beta/\dot{\gamma} = [\eta]\eta_s M/RT \tag{2}$$

Here η and η_0 are the viscosity at finite concentration at a finite shear rate $\dot{\gamma}$ and zero shear rate, respectively, and $[\eta]$ and $[\eta]_0$ are analogous quantities for the intrinsic viscosity. Other parameters are solvent viscosity η_s, polymer molecular weight M, concentration (g/cm^3) c, gas constant R, and absolute temperature T. From the definition of intrinsic viscosity, it is evident that eq 1 and 2 are equivalent reduction factors in the limit of low concentration. Recent experimental work[11,12] has shown that all theories extant are inadequate for describing the non-Newtonian behavior of the intrinsic viscosity.

The present work is concerned with the moderately concentrated to the undiluted state for polymer molecules. Bueche[2] has argued that a macromolecule under these conditions should act as a free-draining molecule and that theories derived for the extremely dilute case should hold here also (so long as entanglement coupling is absent). For the undiluted polymer, η_s is zero and $c = \rho$, the density of the melt, in eq 1 for the Rouse terminal relaxation time. Although, as mentioned above, the theories leading to a non-Newtonian viscosity have been criticized on physical grounds and are recognized here as being incorrect, they will be used for comparison with the experimental results. The justification for this is that no correct theory is available and that the form of the viscosity functions does tend to reproduce the "kinetic stiffness" expected of real polymer chains. Of particular interest is the possibility of the use of a single parameter τ_R for correlation of all the reduced viscosity data. Although predicted by the (incorrect) theories and suggested earlier by Peterlin,[13] no experimental verification has been published. In the case of the non-Newtonian intrinsic viscosity a single parameter is not sufficient.[11,12]

Opposed to these theories was evidence that non-Newtonian flow only occurred with high molecular weight, entangled polymers. Extrapolations of viscosity data as a function of molecular weight measured at constant shear rate or constant shear stress yielded a family of apparently straight lines which intersected at a molecular weight approximately equal to the break in the log η_0 − log M curve.[14-16] It was thus argued that entanglement coupling was a prerequisite for non-Newtonian flow to occur. Subsequent analyses[17,18] showed that the straight lines were in reality curves which approached the log η_0 − log M line asymptotically but did not resolve the question of the reality of nonlinear flow in polymers having no entanglements. The present study was designed to test this latter point.

Experimental Section

For this study a series of nonentangled "monodisperse" polystyrenes was used. The criterion of entanglement for the melts was that the molecular weight should be below M_c, the break point in the plot of log η_0 *vs.* log M, since M_c is the lowest molecular weight for an effect of entanglements to be seen on the Newtonian viscosity. For the moderately concentrated solutions, Fox and Allen[19] have shown that the break point in a plot of log η_0 against

---

[1] Address correspondence to The Institute of Paper Chemistry, Appleton, Wis. 54911.

[2] F. Bueche, *J. Chem. Phys.*, **22**, 1570 (1954).

[3] T. Takemura, *J. Polym. Sci.*, **27**, 549 (1958).

[4] Y.-H. Pao, *J. Chem. Phys.*, **25**, 1296 (1956); *J. Polym. Sci.*, **61**, 413 (1962).

[5] B. H. Zimm, *J. Chem. Phys.*, **24**, 269 (1956).

[6] M. Fixman, *ibid.*, **45**, 793 (1966).

[7] P. E. Rouse, Jr., *ibid.*, **21**, 1272 (1953).

[8] A. Peterlin and M. Copic, *J. Appl. Phys.*, **27**, 434 (1956).

[9] A. Peterlin, *J. Chem. Phys.*, **33**, 1799 (1960).

[10] R. Cerf, *Advan. Polym. Sci.*, **1**, 382 (1958).

[11] I. Noda, Y. Yamada, and M. Nagasawa, *J. Phys. Chem.*, **72**, 2890 (1968).

[12] H. Suzuki, T. Kotaka, and H. Inagaki, *J. Chem. Phys.*, **51**, 1279 (1969).

[13] A. Peterlin, "Proceedings of the 2nd International Congress on Rheology, Oxford, 1953," Butterworths, London, 1954, p 343.

[14] E. B. Bagley and D. C. West, *J. Appl. Phys.*, **29**, 1511 (1958).

[15] R. S. Porter and J. F. Johnson, *Trans. Soc. Rheol.*, **7**, 241 (1963).

[16] R. S. Porter and J. F. Johnson, *ibid.*, **6**, 107 (1962).

[17] E. A. Collins and W. H. Bauer, *ibid.*, **9** (2), 1 (1965).

[18] R. A. Stratton, *J. Colloid Interface Sci.*, **22**, 517 (1966).

[19] T. G. Fox and V. R. Allen, *J. Chem. Phys.*, **41**, 344 (1964).

log M for solutions of constant polymer volume fraction ϕ_2 occurs at $\phi_2 M = M_c$, independent of volume fraction. The solutions in this study have $\phi_2 M < M_c$ and hence should be free from entanglement effects.

Although the solutions show no entanglement coupling effects, there is considerable interpenetration of the polymer coils as calculated by Simha and coworkers. They showed[20] that if there is no contraction of the coil with increasing concentration and hexagonal close packing is assumed, interpenetration will occur for concentrations greater than $1.08/[\eta]$. All of the present solutions exceeded this criterion by at least a factor of 5. Thus, the local environment of a polymer segment is composed of both solvent and polymer segments of neighboring coils.

Anionically polymerized polystyrenes were obtained from two sources. One series (S103, S109, S108) was generously furnished by the late Dr. H. McCormick of the Dow Chemical Co. The others were purchased from Pressure Chemical Co., Pittsburgh, Pa., and are designated by their lot number. The Dow samples have been previously characterized[21] with respect to molecular weight, and the weight-average values are given in Table I. The values for $\langle M \rangle_w$ for the Pressure Chemical Co. samples in Table I are those furnished by the producer and determined at the Mellon Institute.

A portion of sample 3a was fractionated using benzene as solvent and methyl ethyl ketone as nonsolvent. The center cuts comprising about one-third of the total sample were used to make up the sample designated as 3a(F). The fraction had a viscosity-average molecular weight[21] of 4.08×10^5.

Aroclors 1248, 1254, and 1260 were kindly furnished by Mr. R. W. Ehrhardt of Monsanto Chemical Co. Di-2-ethylhexyl phthalate has been previously used[22] as a viscous Θ solvent for polystyrene at 12°. More recent information[23] published after the present measurements were taken indicates that the Θ temperature is 22°. Solutions were made up by slowly stirring weighed mixtures of polymer and solvent at 100° until solution was complete. Densities of the Aroclors were measured pycnometrically; that of DOP was taken from Birnboim.[24] Concentration c in grams of polymer per cubic centimeter of solution was calculated from the densities of polymer and solvent assuming additivity of volumes.

The viscosity of the undiluted polymers of molecular weights 10,500 and 19,800 was measured in a nitrogen gas driven capillary rheometer at 127 and 136°, respectively. Three dies having length-to-diameter ratios of 19.49, 6.68, and 3.80 and radii of 0.0215 in. were used. Die-swell data were obtained by measuring the extrudate diameter to 0.0001 in. with a micrometer. The measurement was taken 0.25 in. from the end so that sagging due to gravity did not influence the results. Subsequent annealing of the extrudates above T_g did not increase the amount of die swell. The rheological properties of the solutions were studied using a Weissenberg rheogoniometer (cone and plate viscometer). Some creep and creep recovery measurements were performed on the low molecular weight undiluted polymers using a modification of the rheogoniometer described elsewhere.[25]

Gel permeation chromatography measurements were carried out on sample 2a by Dr. Jack Q. Cazes and Mr. Russ Dobbins. A Waters analytical GPC unit which had been calibrated with anionically polymerized polystyrenes was operated at 40° using tetrahydrofuran as solvent.

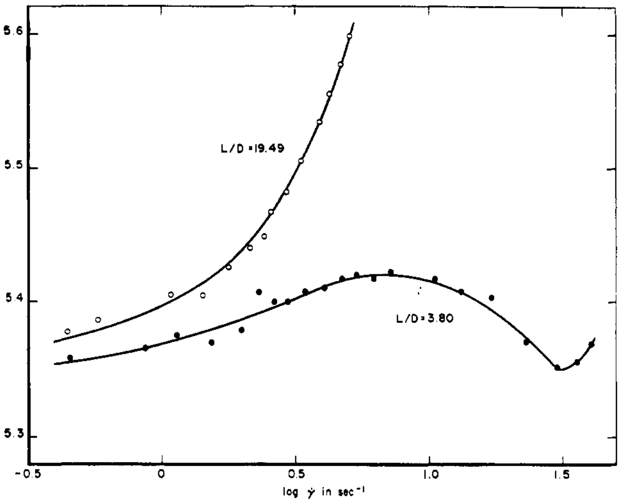

Figure 1. Logarithmic plot of viscosity against shear rate for sample 2a at 136° using capillaries with the indicated length to diameter ratios.

TABLE I
RHEOLOGICAL AND ROUSE THEORY PARAMETERS

Sample	$\langle M_w \rangle \times 10^{-4}$	Solvent	Temp, °C	c, g/cm³	Log η_0	Log $\dot{\gamma}^*$	Log τ_R
3a	39.4	48[a]	25	0.0569	2.02	1.60	−1.73
		48	25	0.0708	2.26	1.39	−1.59
		48	25	0.0836	2.54	1.19	−1.38
		54[b]	25	0.0604	3.40	0.25	−0.38
		60[c]	35	0.0628	4.90	−1.12	1.09
		DOP[d]	12	0.0647	1.92	1.80	−1.97
3a(F)	40.8	48	25	0.0944	2.48	1.28	−1.50
S103	11.7	48	31	0.1144	1.99	2.29	−2.62
		DOP	12	0.1150	1.83	2.37	−2.78
S109	17.9	48	31	0.1144	2.14	2.13	−2.29
		DOP	12	0.1150	2.03	2.19	−2.19
S108	24.2	48	25	0.1240	2.82	1.25	−1.50
		48	10	0.1252	4.18	−0.11	−0.11
		48	25	0.0840	2.19	1.75	−1.97
7a	5.05	48	25	0.524	6.54	−1.10	0.91
		48	40	0.521	5.00	0.44	−0.65
2a	1.98	None	136	1.007	5.38	0.96	−1.07
8a	1.05	None	127	1.011	5.44	1.25	−1.27

[a] Aroclor 1248. [b] Aroclor 1254. [c] Aroclor 1260. [d] Di-2-ethylhexyl phthalate.

Results

Melts. The theories being utilized[2–4] all predict the decrease in viscosity to occur at a reduced shear rate $\dot{\gamma}\tau_R$ of about unity. To attain such magnitudes with low molecular weight polymers without employing very high shear rates, it is necessary to increase the viscosity. This can be simply done by lowering the temperature and working in the present case of $T - T_g \sim 40°$. In this region, certain phenomena occur which are negligible under the usual high-temperature conditions of viscosity measurement. Figure 1 presents double logarithmic plots of viscosity against shear rate for sample 2a using a short die and a long die. At low shear rates the viscosity increases dramatically, while at higher shear rates two factors affecting the magnitude of the viscosity in opposite senses seem to be at work. Such an effect has been noted previously by Ballman.[26] Penwell and Porter[27]

---

(20) S. G. Weissberg, R. Simha, and S. J. Rothman, *J. Res. Nat. Bur. Stand.*, **47**, 298 (1951); R. Simha and J. L. Zakin, *J. Chem. Phys.*, **33**, 1791 (1960).

(21) L. A. Papazian, *Polymer (London)*, **10**, 399 (1969).

(22) J. E. Frederick, N. W. Tschoegl, and J. D. Ferry, *J. Phys. Chem.*, **68**, 1974 (1964).

(23) G. C. Berry, *J. Chem. Phys.*, **46**, 1338 (1967).

(24) M. H. Birnboim, Ph.D. Thesis, University of Wisconsin, 1961.

(25) R. A. Stratton and A. F. Butcher, *J. Polym. Sci., Part A-2*, **9**, 1703 (1971).

(26) R. L. Ballman, *Nature (London)*, **202**, 288 (1964).

(27) R. C. Penwell and R. S. Porter, *J. Appl. Polym. Sci.*, **13**, 2427 (1969).

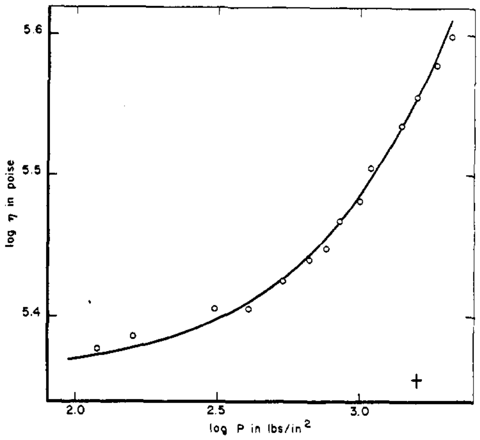

Figure 2. Logarithmic plot of viscosity against pressure for sample 2a at 136° using a capillary with $L/D = 19.49$. Theoretical curve is eq 10.

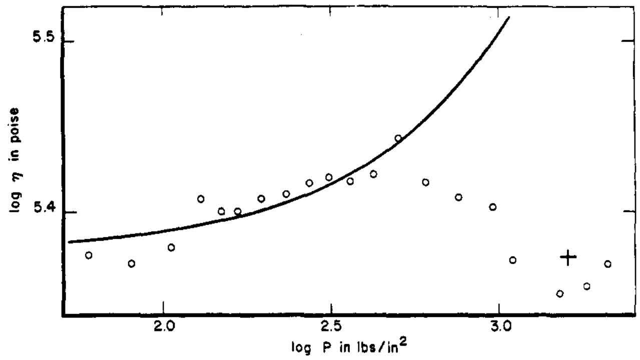

Figure 3. Logarithmic plot of viscosity against pressure for sample 2a at 136° using a capillary with $L/D = 3.80$. Theoretical curve is eq 10.

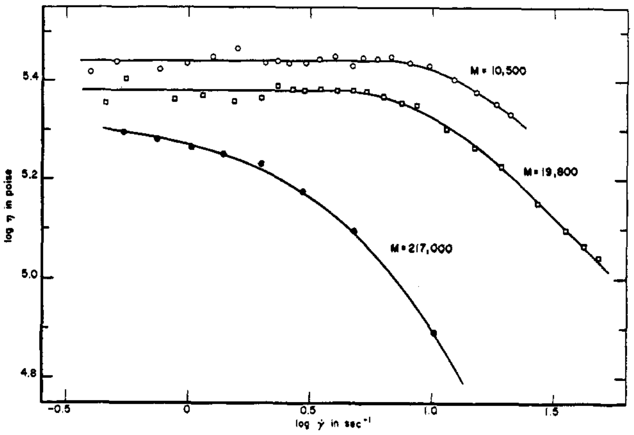

Figure 4. Logarithmic plot of viscosity corrected for pressure effects and nonparabolic velocity profile against shear rate for samples with the indicated molecular weights.

have shown that such viscosity increases do not occur in cone and plate measurements and that the significant parameter is the pressure used in the capillary rheometer.

The effect of pressure on the viscosity of liquids has long been studied.[28] A decrease in free volume occasioned by pressure has often been used as an explanation of this phenomenon. In the vicinity of T_g, where the fractional free volume is small, the effect can be large and has been treated[29] in a manner analogous to the WLF equation. Without regard to the mechanism of the phenomenon, the flow through a capillary of a fluid with pressure-dependent viscosity has recently been treated by Duvdevani and Klein.[30] They consider a particular kind of fluid with viscosity given by

$$\eta(\dot{\gamma}, P) = \eta(\dot{\gamma}, 0)\exp(bP) \tag{3}$$

where $\eta(\dot{\gamma}, P)$ is the viscosity at pressure P and shear rate $\dot{\gamma}$, $\eta(\dot{\gamma}, 0)$ is the viscosity at zero (effectively ambient) pressure, and b is the pressure coefficient. Equation 3 has been found to hold for polystyrene by Maxwell and Jung.[31] For the case of isothermal, incompressible, laminar, Newtonian flow in a capillary with the pressure equal to zero at the exit, Duvdevani and Klein find at the exit

$$PR/2L\dot{\gamma} = \eta(\dot{\gamma}, 0)\mathrm{f}(bP) \tag{4}$$

$$\mathrm{f}(bP) = [bP\exp(bP)]/[\exp(bP) - 1] \tag{5}$$

where R and L are the radius and length of the capillary.

The incompressibility assumption is valid because the change in volume at the pressures used was less[32] than 1%. The left-hand side of eq 4 is the experimentally measured quantity and is just the viscosity calculated using Poiseuille's law. For a Newtonian fluid $\eta(\dot{\gamma}, 0)$ is a constant and the left-hand side and f(bP) should have the same shape. Accordingly, f(bP) was plotted logarithmically against bP as shown by the smooth curve in Figure 2. The experimental data for the long capillary plotted logarithmically as $PR/2L\dot{\gamma}$ against P were then matched to the theoretical curve by horizontal and vertical shifts. The cross denotes the position of f(bP) = 1 and bP = 1 on the theoretical curve. From its position, the zero shear rate viscosity and b can be determined. The experimental points fit the theoretical curve up to the highest pressure used, 2150 psi. In contrast, the data obtained using the short capillary and shown in Figure 3 deviate markedly beginning about 400 psi. These data scattered more than those in Figure 2 at the low pressures and thus were matched to the theoretical curve by using the value of b determined with the long capillary. Data for both capillaries were taken using the same range of pressures. Deviations from Newtonian behavior occur only above a certain shear rate, as seen in Figure 1, which is beyond the range of the long capillary.

Measurements were made on sample 8a with similar results. The values of b for samples 8a and 2a were 10.7×10^{-3} and 9.2×10^{-3} bar^{-1}, respectively. The viscosity data were corrected for the pressure effect by multiplying $PR/2L\dot{\gamma}$ by 1/f(bP) to obtain $\eta(\dot{\gamma}, 0)$. The Weissenberg correction for nonparabolic velocity profile was then applied to obtain a corrected, pressure-independent viscosity hereafter denoted $\eta(\dot{\gamma})$. On the basis of previous work,[18] end corrections were assumed negligible (but see below). The corrected data are plotted logarithmically in Figure 4 as viscosity against shear rate. A sizable deviation from Newtonian behavior is to be noted. Also shown for comparison are data taken previously[18] on S111 at 183°.

---

(28) P. W. Bridgemen, "The Physics of High Pressure," G. Bell and Sons, Ltd., London, 1952.

(29) J. D. Ferry and R. A. Stratton, *Kolloid-Z. Z. Polym.*, **171**, 107 (1960).

(30) I. Duvdevani and I. Klein, *SPE J.*, **23**, 41 (1967).

(31) B. Maxwell and A. Jung, *Mod. Plastics*, **35**, 174 (1957).

(32) S. Matsuoka and B. Maxwell, *J. Polym. Sci.*, **32**, 131 (1958).

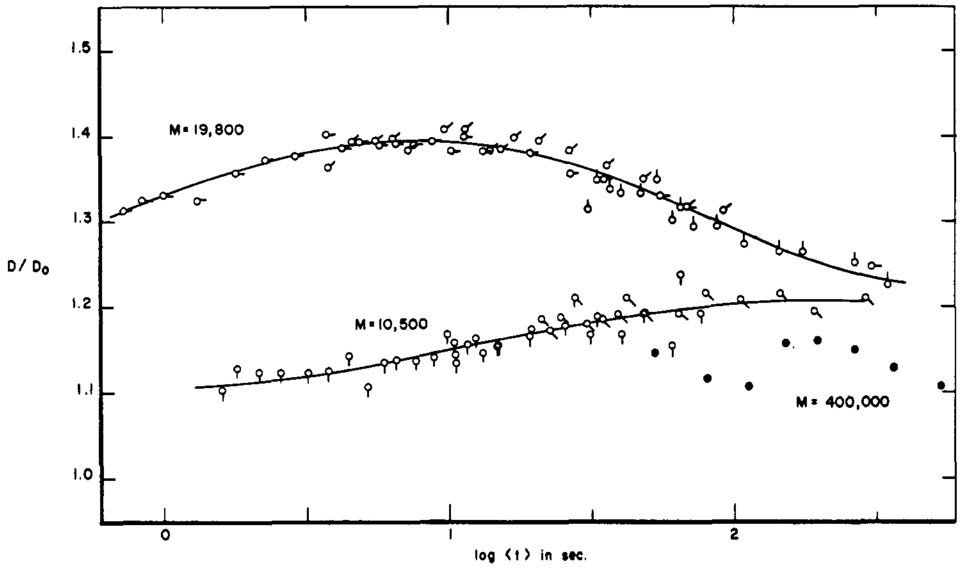

Figure 5. Plot of die swell ratio against logarithm of average residence time in capillary for samples with the indicated molecular weights: pip up, capillary length to diameter ratio 19.49; successive 45° clockwise rotations correspond to L/D of 6.68, 3.80, 19.49, and 3.80; filled in circles, L/D = 19.49.

An anomalously large die swell was noted for these low molecular weight samples. The results are plotted in Figure 5 as swell ratio D/D_0 against the logarithm of the average residence time $\langle t \rangle$. Here D is the extrudate diameter, D_0 is the die diameter, and the average transit time through the die is given by

$$\langle t \rangle = 8L/D_0\dot{\gamma} \tag{6}$$

Data for dies with three different lengths superposed well when plotted in this manner. Die swell for a high molecular weight monodisperse sample also shown for comparison is small as was also the case for the Dow S series samples studied earlier.[18]

Solutions. The shapes of the viscosity–shear rate plots were virtually the same for all solutions. For purposes of comparison, it is of value to choose one sample as a reference and match the data for other samples to it. Because the shape of the flow curves of the three theories being utilized is virtually the same for the initial 20% drop in viscosity, the shear rate $\dot{\gamma}^*$ at which a 15% drop in viscosity was experienced was determined for each sample by noting where the corresponding point on the reference sample fell during the matching process. Employing a reference sample for determination of this characteristic shear rate has the advantage of using all the points of the flow curve for the fitting with concomitant increase in precision rather than stressing those around 15% viscosity loss. The molecular weights, solvents, concentrations, zero shear rate viscosities, and characteristic shear rates γ^* are listed in Table I for the solutions and the undiluted polymers. The latter were also matched to the reference, sample 7a, at a concentration of 0.524 g/cm³ at 25°. Superposition of all the data including the melts was very good over the whole range of shear rates.

Discussion

Dependence on Concentration. According to the several theories mentioned above, data for all samples should fall on a single curve when plotted as $\eta(\dot{\gamma})/\eta_0$ against reduced shear rate $\dot{\gamma}\tau_R$. This implies, using the expression in eq 1, that

$$\dot{\gamma}^* = A/\tau_R = A\pi^2 cRT/6\eta_0 M \tag{7}$$

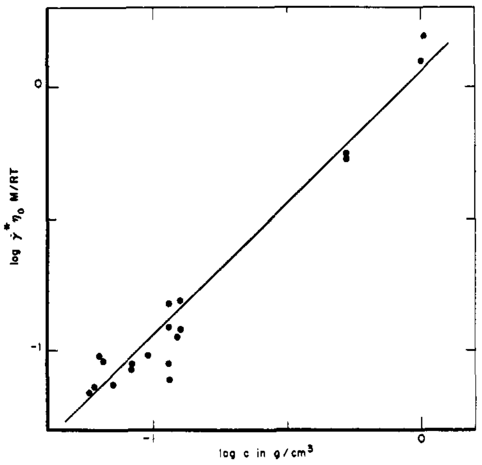

Figure 6. Logarithmic plot of shear rate reduced for viscosity, molecular weight, and temperature against concentration for data in Table I. Line is drawn with theoretical slope of 1.

where A is the theoretical value of $\dot{\gamma}\tau_R$ at η/η_0 = 0.85 and depends upon which theory is used. The contribution of the solvent viscosity to the relaxation time τ_R has been dropped because it is negligible for the solutions under present study. To check the validity of the form of the relaxation time, $\dot{\gamma}^*\eta_0 M/RT$ was plotted logarithmically against c as shown in Figure 6. The straight line drawn with slope 1 appears to be a reasonable fit to the data. The characteristic relaxation time varies inversely as the first power of the concentration.

Dependence on Molecular Weight. To determine the variation of $\dot{\gamma}^*$ with molecular weight, the data were plotted according to eq 7 as $\dot{\gamma}^*\eta_0/cRT$ against M. The double logarithmic plot is shown in Figure 7, where the straight line has been drawn with slope −1. This confirms the first power dependence on molecular weight of the characteristic relaxation time and disagrees with previous work[18] on polystyrene samples with entanglement coupling. For the latter systems a molecular weight exponent of 0.75 was found. This implies a different mechanism for the non-Newtonian behavior in the two cases.

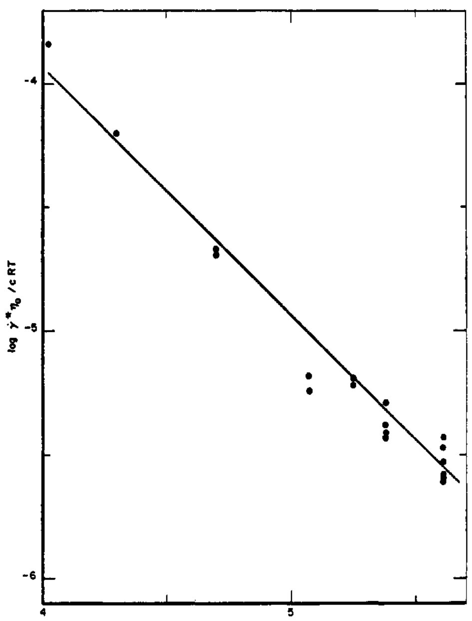

Figure 7. Logarithmic plot of shear rate reduced for viscosity, concentration, and temperature plotted against molecular weight for data in Table I. Line is drawn with theoretical slope of −1.

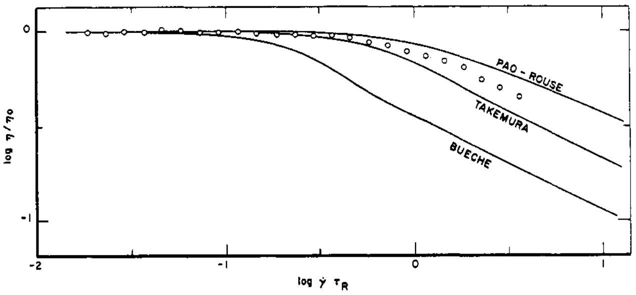

Figure 8. Logarithmic plot of reduced viscosity plotted against reduced shear rate showing predictions of three theories and experimental data on sample 7a (0.524 g/cm^3, 25°).

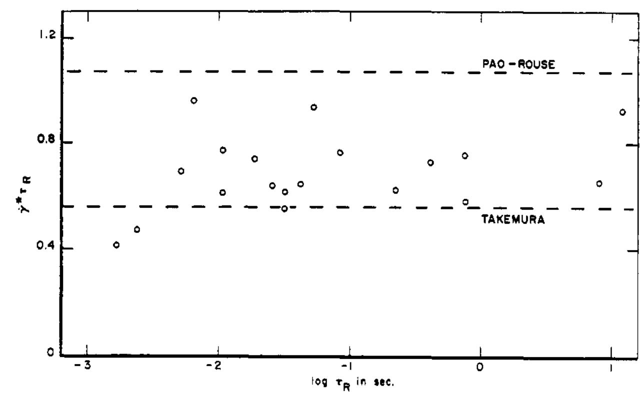

Figure 9. Plot of reduced characteristic shear rate against logarithm of Rouse terminal relaxation time for data in Table I. Magnitude of $\dot{\gamma}^*\tau_R$ predicted by two theories shown by dashed lines.

Experimental Fit of Theories. Qualitatively, all three theories predict the general shape and position on the reduced shear rate axis to within an order of magnitude of the non-Newtonian viscosity of these systems. This is shown in Figure 8, where the reduced viscosity $\eta(\dot{\gamma})/\eta_0$ is plotted logarithmically against the reduced shear rate for the three theories and the data points for the sample (7a, 0.524/cm^3, 25°) used as a reference above. The Bueche and the Takemura curves were drawn using published values;[33,34] the latter is identical with the Rouse function for $\eta'(\omega)$. The Pao theory with Rouse distribution of relaxation times[35] was evaluated by computer. Several features are of interest in this plot. All the theories predict a limiting slope of $-1/2$, which is in agreement with the data presented here, although the latter do not extend a great distance into this terminal slope region. Such behavior is again at variance with previous results[18] on entangled polymers, where a limiting slope of −0.82 was obtained, with the implication of a different mechanism for the two sets of nonlinear phenomena. Bueche's theory predicts non-Newtonian viscosities at reduced shear rates a factor of 4 or 5 smaller than experimentally observed. Because the other two theories predict results somewhat closer to reality, they only will be considered further.

A comparison of all the samples with the theories is shown in Figure 9. Here $\dot{\gamma}^*\tau_R$ is plotted linearly against the logarithm of the Rouse terminal relaxation time. The reduced shear rates for a 15% decrease in viscosity, *i.e.*, the quantity *A*, for the two theories considered are shown by dashed lines. The experimental points generally fall between the two theoretical values, with perhaps some tendency to be nearer the Takemura value. Over a range of four decades of characteristic relaxation time, there is no trend. The results for the three solutions using Θ solvent conditions range from 0.41 to 0.96 again with no trend. The fractionated sample 3a(F) has a value of $\dot{\gamma}^*\tau_R$ of 0.61 or about the average of all the data. The two melts and the solutions all fall in the same range.

From these observations it appears that either the Takemura or the Pao–Rouse theory may be used to predict the magnitude of the non-Newtonian viscosity of nonentangled monodisperse polymer melts or moderately concentrated solutions to within better than a factor of 2. The shape of the theoretical flow curves is qualitatively the same as that observed experimentally.

Non-Newtonian Viscosity of Entangled *vs.* Nonentangled Systems. As pointed out above, there are two distinguishing features in the flow behavior of polymers with and without entanglement coupling: (1) the dependence of the characteristic relaxation time on molecular weight and (2) the limiting high shear rate slope in a logarithmic plot of viscosity against shear rate. In another respect, the two kinds of systems are similar, *viz.*, the region of reduced shear rate where non-Newtonian flow commences.

Based on Bueche's original theory,[2] the Bueche–Harding[36] semiempirical approach has enjoyed a certain amount of success in correlating viscosity behavior with molecular weight. Bueche's terminal relaxation time is retained, but a simple empirical form for the viscosity–shear rate relation is used. This concept has been applied to a number of polymer systems without regard to the presence or absence of entanglement coupling. A great deal of controversy has gone on concerning the proper moment of the molecular weight distri-

---

(33) G. Holden, *J. Appl. Polym. Sci.*, **9**, 2911 (1965).

(34) S. E. Lovell and J. D. Ferry, "Numerical Evaluation of Normal Coordinate Theories for Viscoelastic Properties of Polymers," supplement to *J. Phys. Chem.*, **65**, 2274 (1961).

(35) F. Rodriguez, "Principles of Polymer Systems," McGraw-Hill, New York, N. Y., 1970, p 168.

(36) F. Bueche and S. W. Harding, *J. Polym. Sci.*, **32**, 177 (1958).

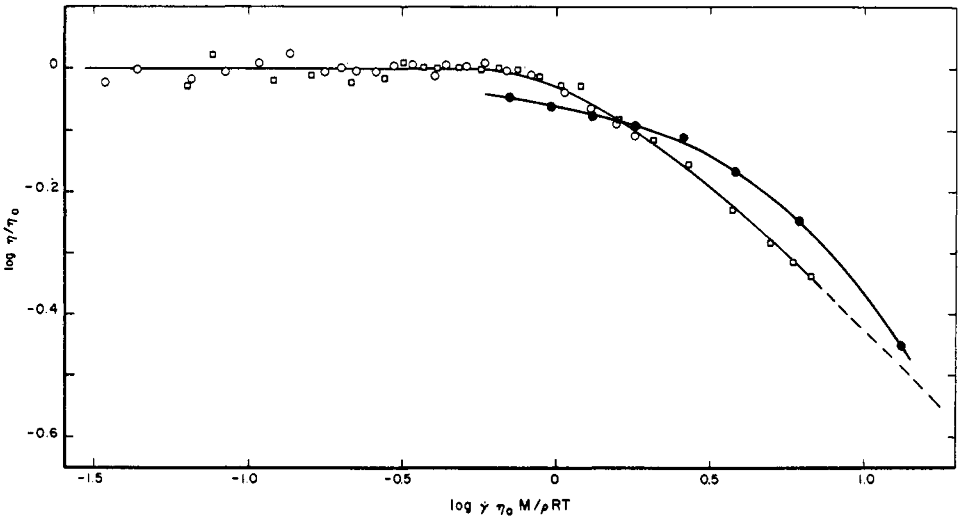

Figure 10. Logarithmic plot of reduced viscosity plotted against reduced shear rate for the data of Figure 5 with the same molecular weight key.

bution to be used for the M in eq 1 for polydisperse materials. With the finding[18] of the fractional exponent of M for entangled systems, the application of the Bueche–Harding approach to these polymers is vitiated. Why then, the apparent success found in the literature? If the data of Figure 4 are plotted on reduced coordinates, the answer becomes obvious, as shown in Figure 10, where reduced viscosity is plotted against reduced shear rate. This procedure superimposes the data for the low molecular weight samples very well, as would be expected from the findings above. The method fails for the entangled polymers.[18] Although the non-Newtonian flow occurs in the same region of reduced shear rate, the shape of the curve is entirely different. However, the very fact that the nonlinear deviation coincidentally takes place in the same range of reduced shear rates accounts for the success of the Bueche–Harding approach; molecular weights for entangled polymers in the usual range ($1–5 \times 10^5$) may be calculated using eq 1 without too much error.

Die Swell. The large die swell, particularly for sample 2a, indicates a highly elastic material. However, on the basis of measurements by Plazek and O'Rourke[37] of the steady-state compliance J_e^0 of monodisperse polystyrenes of similar molecular weight, a rather inelastic polymer would be expected with concomitant little or no die swell. Professor Plazek suggested[38] that the explanation might lie in the contamination of the monodisperse sample with a very small amount of high molecular weight polymer. The addition of small amounts of high molecular weight material to a polymer of much lower molecular weight is well known to greatly enhance the latter's elasticity.

To prove that the die swell was indeed due to an anomalously large elasticity and not to some phenomenon encountered only in a capillary, creep recovery measurements were made in a cone and plate geometry. The steady-state compliance J_e^0 decreased monotonically from 5.7×10^{-5} to 0.95×10^{-5} cm^2/dyn as the shear stress was increased incrementally from 190 to 1.8×10^4 dyn/cm^2. For an uncontaminated sample, the steady-state compliance would be independent of shear stress and equal to about 2×10^{-7} cm^2/dyn.[28] Thus, sample 2a is 50–300 times as elastic as would be expected. The maximum in Figure 5 for this sample can now be rationalized. In general, the die swell, being a measure of the recoverable shear strain, should increase with increasing shear stress or, equivalently in the present case, with decreasing residence time. This expectation is borne out by the results at long residence times. However, at higher shear rates the residence time is too short for the polymer molecules to attain the maximum recoverable deformation and a smaller die swell is observed. A measure of the time required for maximum deformation is given by the product of viscosity and steady-state compliance which has the significance of an average relaxation time for the system. At a shear stress of 2×10^4 dyn/cm^2, ηJ_e^0 is 2.2 sec. Since a period of several relaxation times is necessary to complete a process, the estimated time for maximum deformation is in good agreement with the position of the maximum on the residence time axis. The agreement may only be fortuitous, however, because the maximum in Figure 5 occurs at shear stresses around 10^6 dyn/cm^2, and it is not possible to measure J_e^0 at this stress level nor to estimate it from the data at the lower stresses. An upper limit 9×10^{-6} used in the calculation above can only be placed on it.

A test to determine whether the enhanced elasticity was due to a high molecular weight component was performed using gel permeation chromatography. On ordinary sensitivity, only a slight wiggle in the base line at higher molecular weights was seen. Upon increasing the sensitivity by a factor of 8, a separate peak was observed at a molecular weight of 7×10^6. The concentration based on area under the peak was 0.3%. This finding confirms the origin of the unexpectedly large elasticity and emphasizes the role of very small amounts of high molecular weight polymer on the rheological behavior of polymer melts and solutions.

The presence of the large die swell brings into question the assumption that end corrections to the shear stress are negligible for sample 2a. The end correction is another manifestation of a material's elasticity,[39] and if not accounted for can cause the viscosity to appear larger than reality. The inability to measure the steady-state compliance at the shear stresses used with the capillary rheometer obviates the possibility of calculating the magnitude of the end correction by

---

(37) D. J. Plazek and V. M. O'Rourke, *J. Polym. Sci., Part A-2*, **9**, 209 (1971).

(38) D. J. Plazek, private communication.

(39) W. Philippoff and F. H. Gaskins, *Trans. Soc. Rheol.*, **2**, 263 (1958).

employing the equation of Philippoff and Gaskins.[39] The conclusion to be drawn is that the flow curves of Figure 4 may be in slight error if the end corrections are nonnegligible, and in this case the samples 2a and 8a would be slightly more non-Newtonian.

Acknowledgments. The author wishes to express his thanks to Mr. Allan F. Butcher for his painstaking care in obtaining the data discussed in this report. Professor Donald J. Plazek's helpful discussions and suggestion of the origin of the anomalous die swell are gratefully acknowledged.

Analysis of Polydisperse Systems at Sedimentation Equilibrium. II. Single Components in Mixed Solvents[1]

Arthur Rosenthal

Chemistry Department and Interdepartmental Committee on Biochemistry,
State University of New York, Albany, New York 12203. *Received June 30, 1971*

ABSTRACT: A mathematical function is proposed for the description of preferential interactions of macromolecules with the components of mixed solvents. The function is highly flexible, permitting sufficient scope to encompass many of the forms of interaction previously reported experimentally. Based on this model, an analytical procedure is developed for determining the molecular weight of a polymer and the nature of its interaction with the solvent by means of sedimentation equilibrium studies. Whereas prior applications of the analytical ultracentrifuge to this problem required the assumption of constant preferential interactions, this approach is not so constrained but nevertheless can recognize this effect when it occurs. Although the method has not yet been studied for heterogeneous systems, it is designed to include this possibility as well.

In the first paper of this series,[2] an analytical procedure was presented which had the ability to determine the molecular weights of several independent macromolecular components in simple solvent systems. Such systems are, however, of very limited use in the real world and, accordingly, it is necessary to establish the potential for a good analytical system to be able to operate on realistic solvent systems. The complexity of reality arises in several different ways, of which one, preferential interactions, will be considered in detail in this paper. This phenomenon is a result of the differential binding by a macromolecule of the components of a multicomponent solvent.

The concept of preferential interactions must be distinguished from the more readily appreciated phenomenon of specific binding. The particular type of binding involved is not of direct consequence, nor is the actual magnitude of the binding. What is of concern is the extent to which the composition of the solvent in the immediate environment of the macromolecule is different from the bulk solvent. There, in fact, may be no specific binding as such, but rather a less clear form of intermediate range interaction. Nevertheless, the phenomenon is of great significance.

It has been demonstrated that whenever multicomponent solvents are employed in experiments intended to determine molecular weights by sedimentation techniques, these interactions must be allowed for.[3,4] Several workers[3–7] have also demonstrated the contribution of this phenomenon to light scattering. Thus, it is clear that when determining molecular weights this effect is important. It has also been suggested[4,7] that studies of preferential interactions may be significant toward the understanding of the interplay between solvent composition and protein structure.

There are general treatments of the concept of preferential interactions,[3,4,8] as well as specific experimental considerations of how to estimate their sign and magnitude.[4,7,9–13] For several reasons, generally recognized by their initial proponents, those methods based primarily on the techniques of sedimentation velocity and sedimentation equilibrium are only valid for limited systems in which the samples are homogeneous and the preferential interactions do not depend on the concentration of the cosolute. These techniques really should not be applied when the system under study might not be described within these constraints.[14] In this paper a procedure is presented which, through the use of a generalized computational algorithm, correlates the measured buoyant weights, the solution densities, and the solvent composition to provide estimates for both the molecular weights of the macromolecular components and the preferential interactions between these components and the cosolute as a function of the cosolute concentration. In this initial treatment only solutions of one macromolecular component in two-component solvents will be considered.

Theory

Most of the published considerations of preferential interactions have been based on the general principles of solution thermodynamics. As such, they have been very useful in the development of experimental approaches to the measure-

---

(1) Presented in part at the 162nd National Meeting of the American Chemical Society, Washington, D. C., Sept 1971.

(2) A. Rosenthal, *Macromolecules*, **4**, 35 (1971).

(3) E. F. Casassa and H. Eisenberg, *Advan. Protein Chem.*, **19**, 287 (1964).

(4) A. Rosenthal, Doctoral Dissertation, University of California at Berkeley, 1969.

(5) J. G. Kirkwood and R. J. Goldberg, *J. Chem. Phys.*, **18**, 54 (1950).

(6) W. H. Stockmayer, *ibid.*, **18**, 58 (1950).

(7) S. N. Timasheff and H. Inoue, *Biochemistry*, **7**, 2501 (1968).

(8) V. N. Schumaker and D. J. Cox, *J. Amer. Chem. Soc.*, **83**, 2445 (1961).

(9) E. Reisler and H. Eisenberg, *Biochemistry*, **8**, 4572 (1969).

(10) M. E. Noelken, *ibid.*, **9**, 4122 (1970).

(11) E. P. Kirby Hade and C. Tanford, *J. Amer. Chem. Soc.*, **89**, 5034 (1967).

(12) J. B. Ifft and J. Vinograd, *J. Phys. Chem.*, **70**, 2814 (1966).

(13) H. K. Schachman, "Ultracentrifugation in Biochemistry," Academic Press, New York, N. Y., 1959.

(14) The method discussed by Reisler and Eisenberg[9] is not quite so constrained.